Magnetocrystalline Anisotropy of Magnetic Grains in $Co_{80}Pt_{20}$:Oxide Thin Films Probed by X-ray Magnetic Circular Dichroism

W. Zhang[1], S. A. Morton[2], P. K. J. Wong[1, *], X. F. Hu[1], E. Arenholz[2], B. Lu[3], T. Y. Cheng[1], Y. B. Xu[1, †], and G. van der Laan[4]

[1] *Spintronics and Nanodevice Laboratory, Department of Electronics, University of York, York YO10 5DD, UK*

[2] *Lawrence Berkeley National Laboratory, Berkeley, California 94720, USA*

[3] *Seagate Technology, 47010 Kato Road, Fremont, CA 94538, US*

[4] *Diamond Light Source, Chilton, Didcot OX11 0DE, UK*

Abstract

Using angle-dependent X-ray magnetic circular dichroism we have measured magnetic hysteresis loops at the Co$L_{2,3}$ edges of oxide-doped $Co_{80}Pt_{20}$thin films. The magnetocrystalline anisotropy energy (MAE) of the Co atoms, which is the main source of the magnetocrystalline anisotropy of the CoPt magnetic grains, has beendetermined directly from these element-specific hysteresis loops. When the oxide volume fraction (OVF) is increased from 16.6% to 20.7%, the Co MAE has been found to decrease from 0.117 meV/atom to 0.076 meV/atom.While a larger OVF helps to achieve a smaller grain size, it reduces the magnetocrystalline anisotropyas demonstrated unambiguously from the direct Co MAE measurements.Our results suggest that those$Co_{80}Pt_{20}$:oxide films with OVF between 19.1% and20.7%aresuitable candidates for high-density magnetic recording.

[*] Present address: MESA+ Institute of Nanotechnology, University of Twente, P. O. Box 217, 7500 AE Enschede, The Netherlands.

[†] Corresponding author: yx2@ohm.york.ac.uk

I. Introduction

In order to increase areal densities in hard disk drives and to achieve narrower bit boundaries, it is essential to reduce the magnetic grain size as well as the exchange and/or magnetostatic interaction between the grains [1, 2]. The oxide based grain boundary is effective for this purpose, e.g., oxygen[3] or SiO_2[4] has been composited into CoPtCr to reduce grain size and inter-granular exchange coupling by oxide materials that easily precipitate at the grain boundary.

Girt *et al*. [5]succeeded in isolating the magnetic grains by co-sputtering Co and Pt with nonmagnetic oxide material which serves as a barrier to decouple neighboring grains. With increasing oxide volume fraction (OVF) the magnetic grain size becomes smaller, whileat the same time the magnetocrystalline anisotropy ofthe grains, K_{1g}, was found to be significantly reduced [5]. This result is critical as it suggests that there is a limit for the areal density capability caused by the dilemma between the simultaneous requirements for small grain size and large K_{1g}. The value of K_{1g} is usually *calculated* from the magnetocrystalline anisotropy of the media, K_1, by taking account of the OVF[5, 6]. However, a direct observation and accurateexperimental determinationon the magnetic properties and anisotropies of the magnetic grains is lacking and necessary.

Element-specific X-ray magnetic circular dichroism (XMCD) offers a unique tool for this purpose, as it is capable of measuring the magnetization loops of the individual magnetic element in the magnetic grains, excluding those contributionsfrom the oxide material. In this paper, we measured the angle-dependent XMCD hysteresis loops at the Co $L_{2,3}$edges for a series of $Co_{80}Pt_{20}$:oxide thin films with variable OVF of ~16.6% to 20.7%. In 3*d*-5*d* transition metal alloys, such as Co-Pt, the net magnetization mainly arises from the Co 3*d* magnetic moment, while the Pt 5*d* states carry a small component induced by the 3*d*-5*d*hybridization[7]. This means that despite the important role of the hybridization in giving rise to the giant magnetocrystalline anisotropy of the Co-Pt systems [8], themagnetocrystalline anisotropy energy (MAE)of the Co atoms is still the main source of the K_{1g}[9], which can be determined directly from theelement-specific hysteresis loops.In this work, we

have found that when the OVF increases from 16.6% to 20.7%, the Co MAEdecreases from 0.117 meV/atom to 0.076 meV/atom. In combining with the magnetic measurementsfrom vibrating sample magnetometry (VSM), this work has further suggested that an OVF range of 19.1% - 20.7%issuitable for the magnetic recording.

II. Sample Preparation

We prepared a series of samples, glass/Ta (5 nm)/Ru (13 nm)/$Co_{80}Pt_{20}$ + oxide (total of 13 nm)/C (7 nm), grown by the same method as described in Ref. 5. Thesamples were deposited at room temperature using dc and rf magnetron sputtering in a Unaxis M12 sputter tool with base vacuum below 1×10^{-6} Pa. The magnetic layer of each sample was fixed at the same thickness, formed by co-sputtering Co, Pt, and oxide targets. The CoPt grains were grown on top of Ru grains, with oxide material segregation to the grain boundaries. The oxide co-sputtering power was varied from 5 W to 30 W, which controls theOVF and the grain size, as described below.

III. Results and Discussion

A. TEM measurement of OVF

Plane-view transmission electron microscopy (TEM) was performed to investigate the OVF outcome and corresponding grain sizes. As shown in Fig. 1, the magnetic grains are well isolated by oxide material segregated into the grainboundary.The grain size distribution of thisgranular layer has been fitted with a log-normal distribution and is shown inthe inset, and the meangrain size D is estimated to be 7.8 nm with a standard deviation of ±1.6 nm.

From the TEM analysis, we found that the OVF and grain size dependences are almost linear with the oxide power. As the power increases from 5 W to 30 W, the OVF inthe magnetic layer increases from 16.6% to 20.7%, and the grain size reduces from 10.0 nm to 7.7nm, namely, the grain sizes D are 10.0 nm, 9.5nm, 8.6nm, and 7.7nm, respectively, for the OVF of ~ 16.6%, 17.5%, 19.1%, and 20.7%.

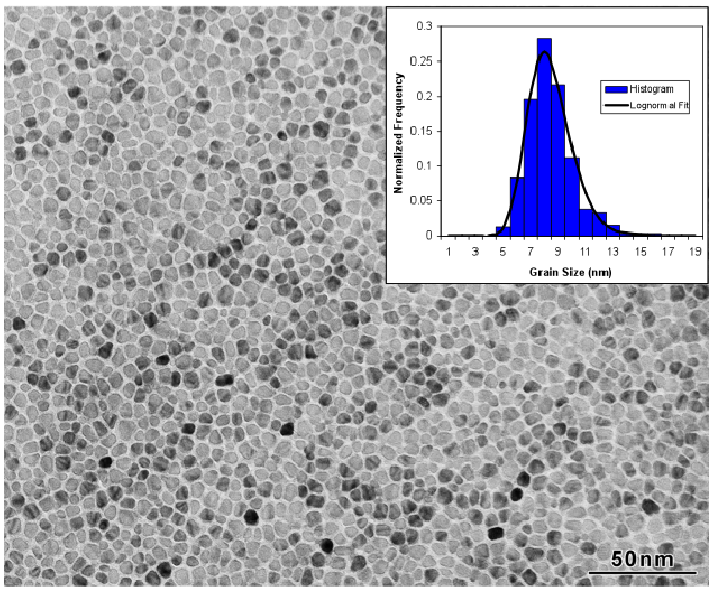

FIG. 1: (Color online) Plane-view TEM image of the granular layer for oxide power of 28 W. Inset: From the grain size distribution of the granular layer the meangrain size *D* is estimated to be7.8 nm.

B. VSM results as a function of OVF

Figure 2(a) shows a typical hysteresis loopof the sample with OVF ~ 16.6% measured by VSM, with the magnetic field applied along the film normal. The coercivity H_C, nucleation field H_N and remanence magnetization $M_r$are marked on the loop. H_N is defined as the field of the intercept between the saturation magnetization level and the tangent at H_C[10], sothat this property describes how well the mediumis able to resist the erasing field from the return pole during the writing process.One more important parameter, remanence squareness S,is defined as the ratio of the remanence magnetization M_r against the saturation magnetization M_S[11], i.e., $S = M_r / M_S$.

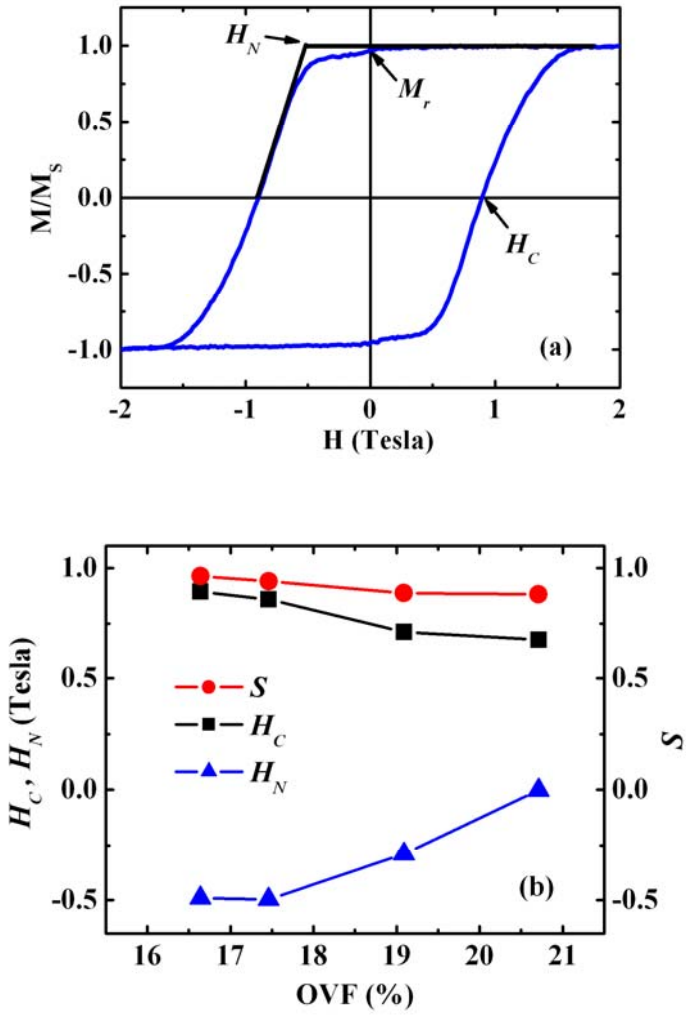

FIG. 2: (Color online) (a) Hysteresis loop measured by VSM when OVF ~ 16.6%, and definition of coercivity H_C, nucleation field H_N and remanence magnetizationM_r;(b) H_C, H_N, and remanence squareness S= M_r /M_S, along the normal direction as a function of OVF.

The trends of H_C, H_N, and $S$are shown in Fig. 2(b) as functions of OVF. For increasing OVF the coercivity $H_C$decreases and the nucleation field $H_N$increases, which suggests that the recording-layer grains are magnetically exchange decoupled and broken up due to enhanced segregation between the media grains.[12]It is commonlyacknowledged

that a large negative $H_N$is essential for the stability of the recorded bit[10], and as one can see in Fig. 2(b), here $H_N$is below zero when the OVF is lower than 20.7%, reaching -0.29 T when OVF ~ 19.1%. The value of S reaches almost 1.0, indicating a high potential of thermal stability of the read-back signal even at low recording density[13]. The decreased S for increasing OVF indicates a reduced intergranular exchange coupling, which is expectedto lead to the formation of smaller domains and in this case themagnetic grains may be reversed individually.[14]

C. MAE as a function of OVF

XMCD measurements were performed on bending magnet beamline 6.3.1 at the Advanced Light Source, Berkeley, usingcircularly polarized X-rays with a degree of circular polarization of ~60%. Using the magnetic field reversal method with a field of ±1.8 T applied parallel to the direction of the incident X-rays, XMCD[15] spectra were recorded at the Co $L_{2,3}$edges[16, 17, 18] and the spin and orbital moments were evaluated by sum rule analysis[19].Figure 3 shows the normalized XMCD spectra measured at the Co$L_{2,3}$ edges atangles γ = 0° (normal) andγ= 60° (grazing) with respect to the surface normal of the sample with 19.1% OVF.

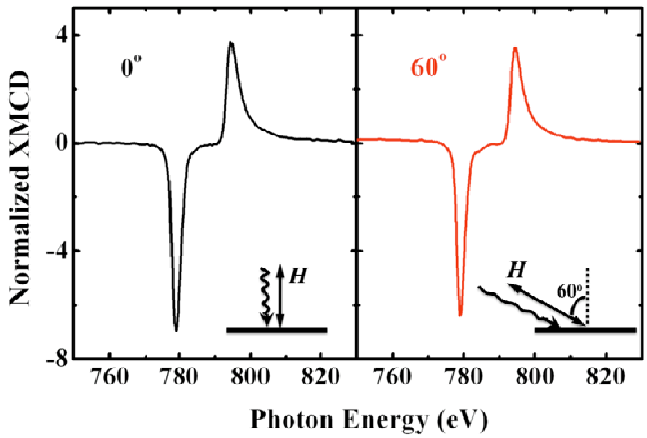

FIG. 3: (Color online) Normalized XMCD spectra at the Co L_3 (~778 eV) and L_2 (~793 eV) edges for the CoPt thin film with 19.1% OVF. Spectra are shown for normal (black) and grazing (red) X-ray incidence relative to the

surface. In both cases the ±1.8 T magnetic field was along the X-ray incidence direction.

We measured element-specific magnetic hysteresis loops by recording the peak height of the CoL_3XMCD signal at ~778 eV dividedby the peak height of the Co L_2 XMCD signal at ~793 eV as a function of the applied magnetic field, forγ = 0° (circles) and 60° (squares), as shown in Fig. 4.The curves show a distinct hysteresis, revealing that the CoPt grains retain grain-grain ferromagnetic alignment at room temperature and all samples exhibit an out-of-plane easyaxis.

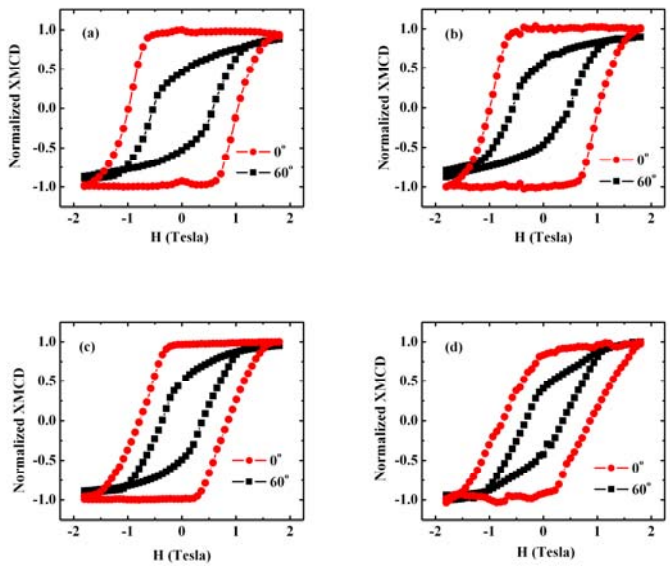

FIG. 4: (Color online) XMCD magnetic hysteresis loop for CoPt films with OVF = (a) 16.6%, (b) 17.5%, (c) 19.1%, and (d) 20.7%, measured at the Co $L_{2,3}$ edges as a function of the applied magnetic field at anglesγ = 0° (red circles) and 60° (black squares).

Figure 5 shows the coercivity of the samples determined from the XMCD hysteresis loops, $H_{C,XMCD}$, at γ = 0° (red closed circles) and 60° (black closed squares). The values and trend are both similar to those measured by VSM, indicating

that the main contribution of the total magnetic moments is due to Co. The theoretical curves of $H_{C,XMCD}$ for $\gamma = 60°$ using the domain wall motion (DWM) model (blue open triangles) and the Stoner-Wohlfarth (SW) rotation model (green open triangles) are plotted for comparison[20]. We see that the experimental data of $H_{C,XMCD}$ at $\gamma = 60°$ almost fully agrees with the calculation using the SW rotation model. However, when the OVF is lower than 19.1%, the magnetization reversal process is slightly towards DWM due to insufficient isolation of the CoPt grains. When the amount of oxide is insufficient to surround the CoPt grains, the oxide may exist as discontinuous sheets or clusters, which behaves as pinning sites and leads to a large coercivity during DWM.[21]When OVF is increased to and larger than 19.1%, more oxide resides around the grain boundaries and forms a quasi-continuous network, whose size might be too large to effectively pin the domain wall, resulting in a smaller $H_{C,XMCD}$ value.[22]

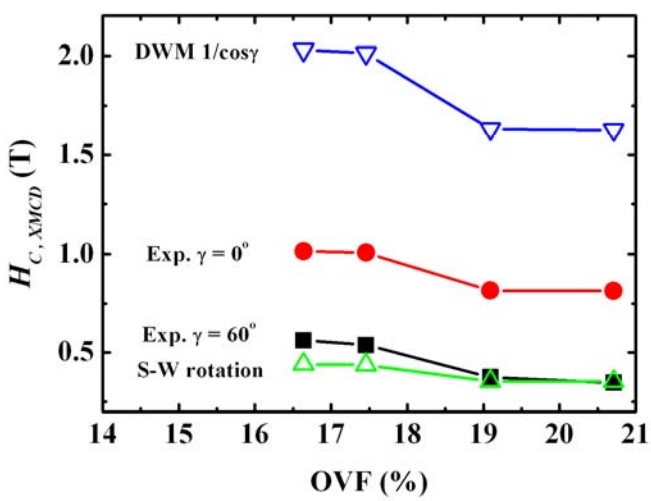

FIG. 5: (Color online) Coercivity measured by XMCD hysteresis loop ($H_{C,XMCD}$) for CoPt films with variable OVF at $\gamma = 0°$ (red closed circles) and 60° (black closed squares).Also plotted are theoretical curves for$H_{C,XMCD}$ at $\gamma = 60°$ using the DWMmodel (blue open triangles) and SW rotation model (green open triangles).

As expected, the reversal process of these samples tends to obey the SW model where the coherent rotation dominates, and the mechanism is the magnetization rotation of each grain[23]. In this case the coercivity may be used to monitor relative changes in the MAE, and therefore one can derive theMAE from the angular dependence of the magnetizationcurves$M(H)$using [24, 25]

$$MAE = \frac{\int_0^{M_S} \left(HdM_{\gamma_1} - HdM_{\gamma_2} \right)}{\sin^2(\gamma_1 - \gamma_2)} \quad (1)$$

where$H$is the applied magnetic field,$\gamma_1 = 0°$and$\gamma_2 = 60°$, and$M_S$is the total magnetic moment estimated at the saturation field using

$$M_S = m_{L,\mathrm{Co}} + m_{\mathrm{Seff,Co}} \quad (2)$$

where$m_{L,\mathrm{Co}}$ and $m_{\mathrm{Seff,Co}}$ are the orbital and spin magnetic moments of Co, respectively. Using the sum rules analysis, we evaluatedthe Co 3d total effective magnetic moment asM_S~1.4 $\mu_B / atom$, which does not vary much with the OVF.

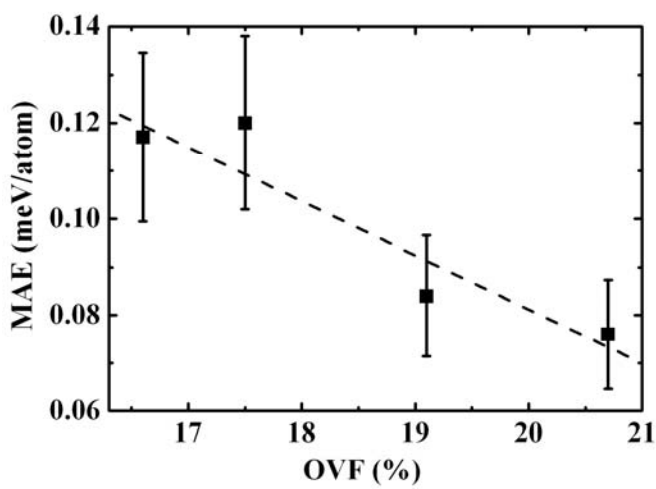

FIG. 6: Co MAE (black squares) vs. OVF determinedfrom Eqs. (1) and (2). Dashed line is a linear fit to the MAE data.

A strong dependence of the MAE on OVF is observed in Fig. 6 with a trend similar to that of the H_C measured by VSM as well as the Co L edges XMCD. The

value of the Co MAE decreases from 0.117 meV/atom to 0.076 meV/atom as the OVF increases from 16.6% to 20.7%, which is consistent with the decreasing trend of K_{1g} with increasing OVF observed in Ref. 5.

V. Conclusions

We have measured for the first time the element-specific hysteresis loopsfor $Co_{80}Pt_{20}$:oxidethin films with perpendicular magnetization using angle-dependent XMCD at the Co$L_{2,3}$ edges. Themagnetization-reversal mechanism of these samples demonstrated to be dominated by the magnetization rotationof each isolated grain, and the Co MAE is evaluated from the angular dependence of $M(H)$in the XMCD hysteresis loops accordingly. When the OVF increases from 16.6% to 20.7%, the Co MAE decreases from 0.117 meV/atom to 0.076 meV/atom. This work has shown that$Co_{80}Pt_{20}$thin filmswith 19.1%-20.7% OVF possessthe most compromisedconditionsfor high-density perpendicular magnetic recording:Namely, sufficiently small and exchange-decoupled magnetic grains witha large MAE and negative nucleation field.

Acknowledgements

We would like to thank Professor H. R. Zhai from Nanjing University in China and Dr. M. P. de Jong from the University of Twente in the Netherlands for valuable discussions, and Mr. Z. Y. Yu from Tsinghua University for TEM data analysis. Thanks also go to Prof. Y. Zhai and Mr. H. B. Huang from Southeast University in China for their kind support of Energy Dispersive X-ray Analysis measurement.

The Advanced Light Source is supported by the Director, Office of Science, Office of Basic Energy Sciences, of the U.S. Department of Energy under Contract No. DE-AC02-05CH11231.

Reference

[1] S. N. Piramanayagam, J. Appl. Phys. **102**, 011301 (2007).

[2] G. A. Bertero, D. Wachenschwanz, S. Mailhota, S. Velu, B. Bian, D. Stafford, Y. Wu, T. Yamashita, and S. X. Wang, IEEE Trans. Magn. **38**, 1627 (2002).

[3] S. Oikawa, *et al*., IEEE. Trans. Magn. **36**, 2393 (2000).

[4] T. Oikawa, *et al*., IEEE. Trans. Magn. **38**, 1976 (2002).

[5] E. Girt, S. Wu, B. Lu, and G. Ju, *et al*., J. Appl. Phys. **99**, 08E715 (2006).

[6] T. Shimatsu, *et al*., IEEE. Trans. Magn. **40**, 2483 (2004).

[7] N. Ishimatsu, *et al*., J. Appl. Phys. **106**, 033902 (2009).

[8] I. V. Solovyev, P. H. Dederichs, and I. Mertig, Phys. Rev. B. **52**, 13419 (2002).

[9] K. H. J. Buschow, *et al.*, J. Magn. Magn. Mater. **38**, 1 (1983); F. Menzinger and A. Paoletti, Phys. Rev. **143**, 365 (1966).

[10] T. Keitoku, *et al*., J. Magn. Magn. Mater. **235**, 34 (2001).

[11] B. Lu, D. Weller, *et al*., IEEE. Trans. Magn. **39**, 1908 (2003).

[12] S. N. Piramagnayagam, K. Srinivasan, Appl. Phys. Lett. **91**, 142508 (2007).

[13] T. Shimatsu, *et al*., J. Magn. Magn. Mater. **235**, 273 (2001).

[14] N. Powers, M. L. Yan, L. Gao, S. H. Liou, and D. J. Sellmyer, J. Appl. Phys. **91**, 8641 (2002).

[15] D. Weller, and J. Stohr, *et al*., Phys. Rev. Lett. **75**, 3752 (1995).

[16] H. A. Durr, S. S. Dhesi, E. Dudzik, D. Knabben, G. van der Laan, J. B. Goedkoop, and F. U. Hillebrecht, Phys. Rev. B **59**, R701 (1999).

[17] E. Dudzik, H. A. Durr, S.S. Dhesi, G. van der Laan, D. Knappen, and J. B. Goedkoop, J. Phys.: Condens. Matter. **11**, 8445 (1999).

[18] N. Weiss *et al.*, Phys. Rev. Lett. **95**, 157204 (2005).

[19] B. T. Thole, P. Carra, F. Sette, and G. van der Laan, Phys. Rev. Lett. **68**, 1943 (1992).

[20] K. K. M. Pandey, J. S. Chen, J. F. Hu, and G. M. Chow, J. Phys. D: Appl. Phys. **42**, 015009 (2009).

[21] D. I. Paul, J. Appl. Phys. **53**, 2362 (1982); M. T. Rahman, C. H. Lai, Y. C. Wu, N. N. Shams, and D. Suess, Appl. Phys. Lett. **91**, 132505 (2007).

[22] Y. C. Wu, L. W. Wang, C. H. Lai, and C. R. Chang, J. Appl. Phys. **103**, 07E140 (2008).

[23] G. Moulas, *et al*., Phys. Rev. B. **78**, 214424 (2008).

[24] R. M. Bozorth, Phys. Rev. **50**, 1076 (1936).

[25] P. Gambardella, A. Dallmeyer, K. Maiti, M. C. Malagoli, S. Rusponi, P. Ohresser, W. Eberhardt, C. Carbone, and K. Kern, Phys. Rev. Lett. **93**, 077203 (2004).

This document was prepared as an account of work sponsored by the United States Government. While this document is believed to contain correct information, neither the United States Government nor any agency thereof, nor the Regents of the University of California, nor any of their employees, makes any warranty, express or implied, or assumes any legal responsibility for the accuracy, completeness, or usefulness of any information, apparatus, product, or process disclosed, or represents that its use would not infringe privately owned rights. Reference herein to any specific commercial product, process, or service by its trade name, trademark, manufacturer, or otherwise, does not necessarily constitute or imply its endorsement, recommendation, or favoring by the United States Government or any agency thereof, or the Regents of the University of California. The views and opinions of authors expressed herein do not necessarily state or reflect those of the United States Government or any agency thereof or the Regents of the University of California.